Why Are Vibrational Lines Narrow in Proteins?

Journal:	*The Journal of Physical Chemistry Letters*
Manuscript ID	jz-2020-01760y.R1
Manuscript Type:	Letter
Date Submitted by the Author:	n/a
Complete List of Authors:	Martin, Daniel; Arizona State University, Physics Matyushov, Dmitry; Arizona State University, School of Molecular Sciences

Why are Vibrational Lines Narrow in Proteins?

Daniel R. Martin[†] and Dmitry V. Matyushov[*,‡]

†*Department of Physics, Arizona State University, PO Box 871504, Tempe, Arizona 85287*

‡*Department of Physics and School of Molecular Sciences, Arizona State University, PO Box 871504, Tempe, AZ 85287-1504*

E-mail: dmitrym@asu.edu

Abstract

Vibrational Stark effect in proteins yields line shifts indicative of strong internal electric fields up to a few V/Å. These values are supported by numerical simulations of proteins. The simulations also show significant breadth of field fluctuations translating to inhomogeneous broadening of vibrational lines. According to fluctuation-dissipation arguments, strong internal fields should lead to broad lines. Experimentally reported vibrational lines in proteins are, however, very narrow. This disconnect is explained here in terms of insufficient (nonergodic) sampling of protein's configurations on the lifetime of the vibrational probe. The slow component of electric field fluctuations in proteins relaxes on the time scale of tens of nanoseconds and is dynamically frozen on the vibrational lifetime.

TOC Graphic

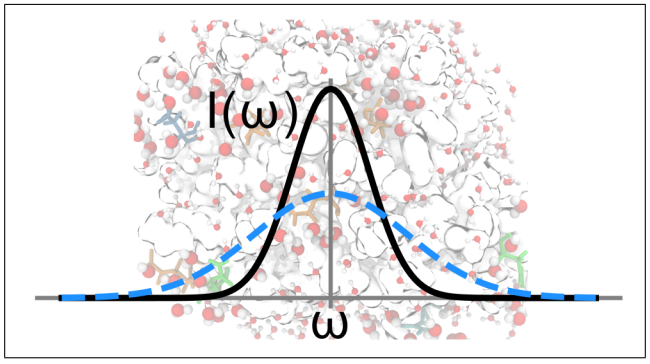

Electrostatics strongly affects protein's ability to catalyze chemical reactions[1] (electrostatic catalysis[2,3]). The importance of electrostatics applies to both the average field inside the protein, which can measure as high as $\sim 10^8$ V/cm,[2–5] and to fluctuations of the electric field. The average electric field promotes redistribution of charge in a chemical reaction toward lowering the activation barrier. In energetic terms, a nonzero average electric field within a protein can lower the energy of the transition state if the substrate is properly oriented in the active site. This is a specific realization of Pauling's mechanism of transition state stabilization[6] by intraprotein electric field. Fluctuations around the average electric field are also important since they modulate energy levels of localized electronic states, promoting tunneling of electrons in individual electron-transfer steps in energy chains of biology. The role of fluctuations is more complex than that of the static field since stronger fluctuations also mean stronger solvation of the localized state and deeper traps to overcome for tunneling (reorganization energy[7]). These fluctuation-dissipation[8] arguments suggest that intense field fluctuations should increase the activation barrier. Hence, an "ideal enzyme" should be viewed as a rigid environment allowing a well-defined directed field to stabilize the activated state, but no field fluctuations. This is clearly not a realistic model of a protein in solution, which shows significant flexibility on a nearly continuous spectrum of relaxation time scales.[9,10]

A possible resolution of the dilemma of deeper traps produced by stronger fluctuations, which is the statement pertinent to linear response theories and fluctuation-dissipation relations,[8] is in separation of relevant time scales. If full sampling of configurations is not allowed on the observation time scale (reaction time or the lifetime of a spectroscopic probe), the fluctuation-dissipation restrictions are lifted. The ensuing separation of the first (averages) and second (fluctuations) statistical moments leads to the catalytic effect, i.e., to lowering of the activation barrier for charge transfer.[11] The conceptual framework leading to this conclusion is the statement that the effective broadening of a localized electronic state observed on a given time scale is lower than one would anticipate if the observation time had been extended to cover all fluctuating degrees of freedom affecting the electronic energy level. Stated this way, this perspective is really an old news for spectroscopy since it goes back to the line broadening function introduced by Kubo and An-

derson.[12,13] The loss of inhomogeneous broadening by a spectroscopic probe due to insufficient sampling of fluctuations, if measured, provides an important insight into both the time scales involved and the breadth of thermal noise. This issue is explored here by modeling broadening of carbonyl vibrations inside the cytochrome *c* (cytC) protein. Vibrational probes inside proteins have demonstrated much narrower lines than in water.[14] We show that insufficient sampling of protein's electrostatic fluctuations on the lifetime of vibrational excitation provides a plausible explanation of this observation.

The standard analysis of vibrational lines anticipates that one can calculate the line shape from modulations of the vibrational transition frequency $\delta\omega$ produced by thermal environment. If the statistics of $\delta\omega$ is Gaussian, the line shape is expressed in terms of the Kubo-Anderson line broadening function[12,13]

$$g(t/\tau) = \kappa^{-2}\left[e^{-t/\tau} + t/\tau - 1\right] \tag{1}$$

Here, τ is the exponential relaxation time of the time autocorrelation function of $\delta\omega(t)$. The parameter[15]

$$\kappa = (\tau\sigma)^{-1} \tag{2}$$

is based on the relaxation time τ and the variance $\sigma^2 = \langle(\delta\omega)^2\rangle$ of the transition frequency ω. It specifies two limits. When $\kappa \ll 1$, the resulting Gaussian line shape is caused by inhomogeneous broadening produced by medium fluctuations. In the opposite limit $\kappa \gg 1$, known as motional narrowing, fast frequency modulation prevents inhomogeneous broadening from happening, leading to an overall Lorentzian line shape.[16]

This broadly accepted picture still involves an assumption often not directly spelled out. In order to reach the limit of inhomogeneous broadening, one still needs to assume that the lifetime of the vibrational state far exceeds time scales of medium fluctuations responsible for the variance σ^2. This is the assumption of ergodicity, or the ability to sample all significant states producing the frequency variance. If this is not the case, the slow modes, which are dynamically frozen on the lifetime of the vibrational probe, should be eliminated from the variance σ^2 by some mathematical

procedure accounting for incomplete sampling. We present here evidence that narrow lines of vibrational probes in proteins are caused by such incomplete sampling. It arises from the lifetime of the vibrational state, which establishes the observation time $\tau_{\rm obs}$, being significantly shorter than the characteristic slow relaxation time of the medium τ_s

$$\tau_{\rm obs} \ll \tau_s \tag{3}$$

The dynamics of electric-field fluctuations inside the protein are characterized here by two decaying exponential functions with the relaxation times τ_a, $a = {\rm f,s}$ with the fast (f) and slow (s) components. Correspondingly, one can write the line shape as a time integral involving the vibrational frequency ω, which is viewed as the deviation from the line maximum not specified here. We instead are interested only in the line shape or, more specifically, in the line width. The line function is then given by the time integral[16,17]

$$I(\omega) \propto \int_{-\infty}^{\infty} dt \exp\left[i\omega t - \sum_{a={\rm f,s}} g_a(t/\tau_i)\right] \tag{4}$$

where each $g_a(t/\tau_a)$ is characterized by the relaxation time τ_a and the variance σ_a^2. These components are assigned based on the time correlation function

$$\langle \delta\omega(t)\delta\omega(0)\rangle = \langle(\delta\omega)^2\rangle \sum_{a={\rm f,s}} A_a e^{-t/\tau_a} \tag{5}$$

The variance of each relaxation component $\sigma_a^2 = \langle(\delta\omega)^2\rangle A_a$ is determined by its weight A_a, $\sum_a A_a = 1$.

Our simulations of the statistics of electric field at a number of sites within the protein have lead to two widely separated line broadening scenarios. We always get the inhomogeneous broadening limit $\kappa_s \ll 1$ for the slow component, but the faster relaxation time often yields κ_f close to unity. The slow component thus contributes to the inhomogeneous Gaussian broadening, but we cannot assign the Lorentzian function to the faster relaxation component. Therefore, the line shape $I(\omega)$

was produced by numerical fitting of the function $\exp[-g_f(t/\tau_f)]$ to a sum of Gaussian functions of t for each set of parameters, with the resulting sum of Gaussians of ω representing the final line-shape function as we discuss in more detail in Supplementary Information (SI).

Equation 4 combines fast and slow relaxation components of the frequency time correlation function merging the homogeneous and inhomogeneous broadening of the vibrational line shape into one line-shape function.[16] This description still does not incorporate the dynamical freezing of the slow modes responsible for inhomogeneous broadening. Phenomenological arguments will be used here to produce a physically motivated solution allowing closed-form description of the vibrational line shape. The arguments are given in both the time and frequency domains.

Since the stochastic process leading to the Kubo-Anderson function is Gaussian, one can apply general properties of the stochastic Gaussian (Ornstein-Uhlenbeck[18]) process[19] anticipating that the Gaussian width broadens with the observation time as

$$\sigma_{\text{obs}}^2 = \sigma_s^2 \left(1 - e^{-2\tau_{\text{obs}}/\tau_s}\right) \tag{6}$$

This effective variance can then be used in the line-shape calculation in place of σ_s^2.

An alternative approach follows from the frequency-domain arguments.[11] One assumes that the power spectrum of vibrational frequency fluctuations is constrained by the medium frequencies exceeding the nonergodic cutoff ω_c. If the relaxation mode is exponential, the effective broadening becomes

$$\sigma_{\text{obs}}^2 = (2\sigma_s^2/\pi)\text{cot}^{-1}(\omega_c\tau_s) \tag{7}$$

We find that adopting $\omega_c = (3\tau_{\text{obs}})^{-1}$ brings eqs 6 and 7 to full agreement when used to produce the line-shape function (see Figure S1 in SI).

To access the statistics and dynamics of $\delta\omega$, we analyzed fluctuations of the electric field at a number of carbonyl groups inside cytC in the oxidized state solvated by TIP3P water. Trajectories for this system were produced by molecular dynamics (MD) simulations as explained in more detail in SI. Electric field from the protein and water was projected on the direction of the carbonyl

bond in 20 amino acids including 5 asparagines (ASN), 3 aspartic acid (ASP) residues, 3 glutamines (GLN), and 9 glutamic acid (GLU) residues (Table S1 in SI). The connection between the projected field $E_{\|}$ and the vibrational frequency was taken from the scaling relation for the vibrational Stark effect calibrated by Boxer and co-workers:[14] $\omega = 0.41E_{\|}$, where ω is in cm^{-1} and $E_{\|}$ is in MV/cm (the tuning rate of 0.61 cm^{-1}/(MV/cm) is used for nitriles[5]). This connection assumes that electric field is the main contributor to the line shift and broadening in polar media. This assessment has been supported by a number of studies, which have also reported more sophisticated maps than the simple choice adopted here.[20,21] With the adopted mapping, we can address only the line width, but not the line skewness.[20]

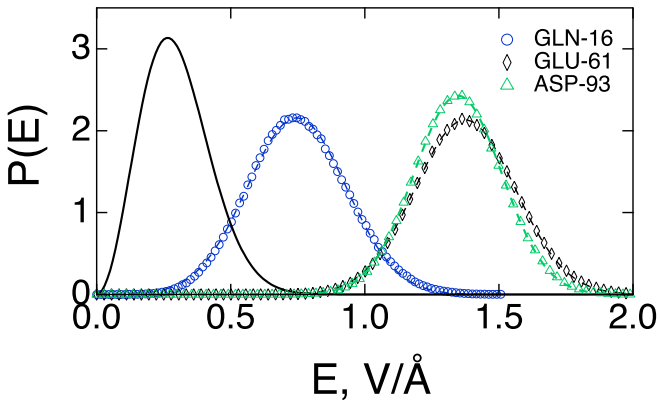

Figure 1: Distribution of the magnitudes of the electric fields at the carbonyl groups in cytC listed in the plot. The dashed lines are Gaussian fits through distributions calculated from MD trajectories. The solid line indicates the Maxwell distribution with the width specific to GLU-61.

The mean projected field and its variance change little among the residues studied, suggesting that the electric field varies little inside the protein. This observation is consistent with the standard ideas of dielectric theories regarding the reaction field inside a dipolar solute.[22] The overall charge of a spherical solute induces a constant solvent potential and no electric field while the solute dipole produces a constant reaction field inside the solute. With the dipole moment of oxidized cytC $M \simeq 238$ D[23] and the radius of $R \simeq 19$ Å, the dielectric estimate for the reaction field $\simeq M/R^3$ yields $E \simeq 0.1$ V/Å. The magnitudes of the field obtained from simulations are about an order of magnitude higher, $E \simeq 1$ V/Å. This result is not unexpected. A number of electrostatic

properties of solvated proteins indicate that screening of electrostatic interactions by the protein hydration layer does not follow the recipes of dielectric theories and is usually much diminished compared to dielectric estimates.[24] The reaction field adds to the intraprotein field due to charged surface residues.

The distribution of the field magnitude E calculated at the carbonyl groups in the laboratory reference frame does not follow the Maxwell distribution and can instead be well approximated by a Gaussian function with a non-zero mean value (Figure 1). The appearance of the mean field magnitude in the distribution implies that the field produced by the protein at a given site is non-zero, and it does not get averaged by protein rotations in the laboratory frame on the simulation time of 250 ns. The projection of the field on the carbonyl direction $E_{\|} \simeq 0.6 - 0.9$ V/Å (Table S1 in SI) is invariant to rotations of the system of coordinates and the corresponding distributions are also well approximated by Gaussian functions.

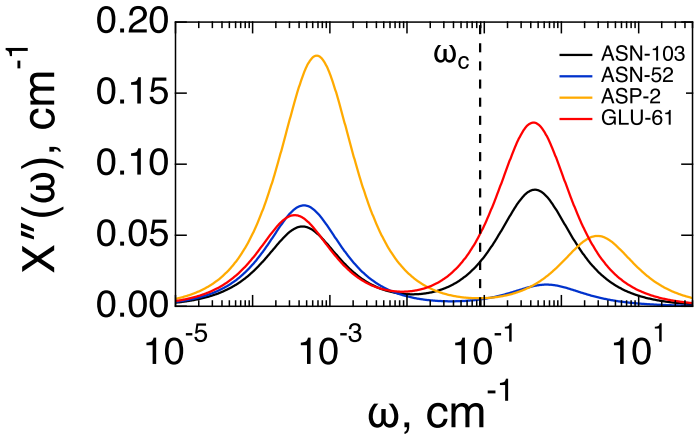

Figure 2: Power spectrum (eq 8) of frequency fluctuations vs ω in cm^{-1}. The vertical dashed line shows the cutoff frequency $\omega_c = (3\tau_{\rm obs})^{-1}$ with $\tau_{\rm obs} = 20$ ps.

Figure 2 shows representative power spectra of frequency fluctuations at carbonyls of the residues listed in the plot. The power spectrum is produced from the two-exponential time correlation function in eq 5. Based on standard rules of linear-response theory, one obtains[25]

$$\chi''(\omega) = \beta\langle(\delta\omega)^2\rangle \sum_{a={\rm f,s}} A_a \frac{\omega\tau_a}{1+(\omega\tau_a)^2} \qquad (8)$$

where the imaginary part of the response function represents the power (loss) spectrum for a specific site. Integration of the slow component of this function at $\omega > \omega_c$ leads to an effective broadening in eq 7 affected by insufficient sampling. It is clear that $\omega_c = (3\tau_{\text{obs}})^{-1}$ (vertical dashed line in Figure 2) much exceeds τ_s^{-1} for the slow component represented by the low-frequency Lorentzian peak in the power spectrum. Therefore, only a small fraction of σ_s^2 contributes to inhomogeneous broadening of the vibrational line. However, the condition $\kappa_s \ll 1$ still applies and the effective inhomogeneous width contributes to the Gaussian component of the overall line shape.

Calculations with the effective broadening by slow medium dynamics either through the Ornstein-Uhlenbeck algorithm (eq 6) or through the frequency cutoff (eq 7) were performed to calculate the effective vibrational linewidth. Figure 3 compares the results of full equilibrium calculations assuming $\tau_{\text{obs}} \to \infty$ with the sampling restriction imposed by $\tau_{\text{obs}} = 20$ ps as found from the population relaxation of carbonyl stretch vibration in the active site of hydrogenase.[26] This time scale is intermediate between longer relaxation times of 50-100 ps in synthetic systems in low-polarity solvents[27] and 3.7 ps found for the lifetime of metallocarbonyls covalently attached to a lysozyme protein.[28] It appears that water provides the dominant relaxation pathway and the observed vibrational lifetime greatly depends on the distance between the vibrational probe and the hydration shell.[17,29] Adopting a shorter lifetime τ_{obs} will make the vibrational lines only narrower. Our calculations are compared to line shapes reported by Boxer and co-workers for the acetophenone vibrational probe inside the hydrophobic core of the protein and in water.[14] Figure 3 shows the calculations for the carbonyl group of ASP-2 of cytC, but the results are overall consistent among all amino acids studied here.

The main result of our calculations is that the nonergodic line shape calculated by reducing the slow-mode broadening to σ_{obs} is consistent with experimental observations of narrow line shapes in the protein's hydrophobic core. Even more strikingly, the full equilibrium line shape assuming $\tau_{\text{obs}} \to \infty$ and $\sigma_{\text{obs}} = \sigma_s$ is consistent with the line broadening observed in pure water (a near coincidence with the experimental results in water in Figure 3 is fortuitous). Therefore, the protein matrix as a source of stochastic noise is not much different from bulk water and in fact allows a very

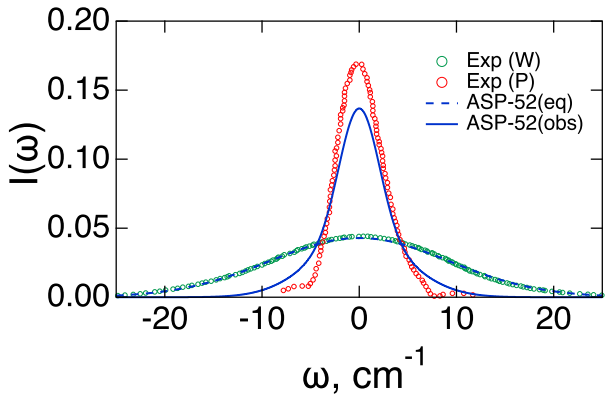

Figure 3: Vibrational line calculated with $\sigma^2_{\rm obs}$ (solid line, "obs") and the full inhomogeneous width σ^2_s (dashed line, "eq"). These calculations are compared to experimental (Exp) vibrational lines of acetophenone vibrational probe in protein (P) and water (W).. [14]

similar amplitude of electrostatic fluctuations. The shielding of electrostatic fluctuations achieved by the protein is not statistical or structural, but dynamical. A protein creates an effectively nonpolar environment for a vibrational probe by slowing down the interfacial dynamics of electrostatic fluctuations.

The time-scale of electric field fluctuations inside a small molecule inserted in the liquid is close to the longitudinal dielectric relaxation time of the liquid. For a spherical molecule, it is given by the dielectric formula accounting for the cavity-field correction [30] of the Debye relaxation time τ_D

$$\tau_E = \frac{3\epsilon_\infty}{2\epsilon_s + \epsilon_\infty}\tau_D \tag{9}$$

where ϵ_s and ϵ_∞ are the static and high-frequency dielectric constants of the solvent. For water with $\tau_D \simeq 9$ ps at normal conditions, one arrives at $\tau_E \simeq 0.3$ ps. Instead of this very fast relaxation indeed recorded by the Stokes-shift dynamics of photoexcited dyes, [31] the long-decay relaxation components of the protein-water interface are much longer, in the range of 6-16 ns (Table S1 in SI).

The relaxation times τ_a are mostly consistent among the residues studied here. On the other hand, the distribution of relative amplitudes of the fast and slow relaxation modes is not entirely uniform (Figure 4, upper panel). The relative importance of the fast relaxation component is affected by the distance between the carbonyl and the hydration shell. One would anticipate that

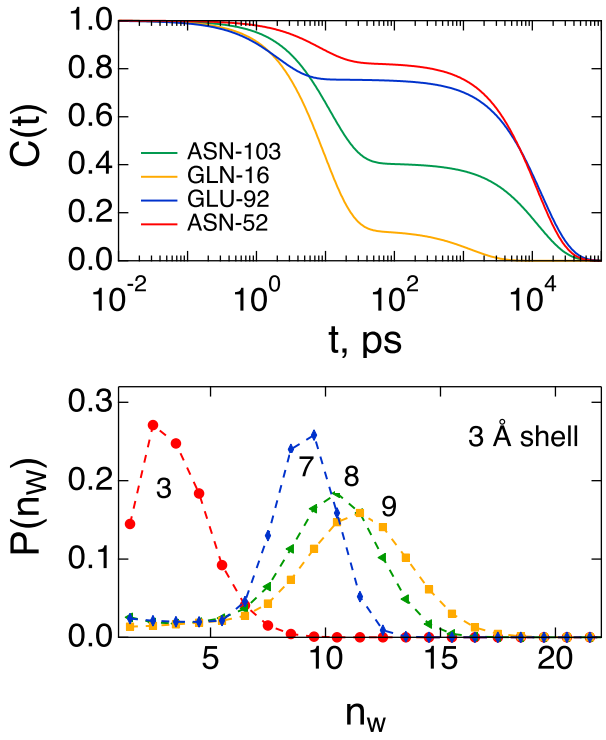

Figure 4: Normalized time correlation function $C(t) = \langle \delta\omega(t)\delta\omega(0)\rangle / \langle (\delta\omega)^2 \rangle$ for different carbonyl groups indicated in the plot (upper panel). In the lower panel, the distribution of the number of waters n_W within the radius of 3 Å from the carbonyl is shown for the same set of residues as in the upper panel. The numbers in the plot list the average values $\langle n_W \rangle$.

carbonyls closer to water would have a larger fraction of the fast component and broader vibrational lines. We in fact find that all residues from our set have some exposure to water. There are, however, differences in the exposure as is seen from the distributions of the number of waters within the radius of 3 Å from a given carbonyl (Figure 4, lower panel). Only a few residues show numbers below 5, and we indeed observe a trend of a larger fraction of the fast relaxation component with increasing the average number $\langle n_W \rangle$ of closest waters. The exact effect of water exposure is hard to model since broadening by faster electric field dynamics can be balanced by a shorter lifetime of the vibrational excitation, also affected by the distance to the hydration shell.[28]

The disruption of the water structure by the heterogeneously charged and topologically irregular[32] surface of the protein leads to relatively insignificant alteration of the single-particle dynamics of water in the hydration shell. The retardation factor for the corresponding relaxation time is within one order of magnitude.[33,34] The fast component of the electric-field dynamics shows about the same retardation factor of about two.[35] However, it is the long-time collective dynamics that are most affected by the protein. The long-time dynamics of the electric field at the protein active site are in the nanosecond domain, as observed experimentally by time-resolved Stokes shift,[36–38] in our previous simulations,[39] and confirmed here with more specific probes at different locations inside the protein. This significant slowing down is also consistent with the collective dynamics of the hydration shell dipole moment of a typical globular protein, also in the range of nanoseconds[40] (cf. to Debye relaxation time of $\simeq 9$ ps for bulk water). A complete physical picture of this phenomenon is not entirely established, but simulations indicate breaking of the protein's hydration shell into slowly relaxing domains with predominantly parallel orientations of water dipoles.[40] Independently of the origin, our results here show that slow dynamics of the electric field, linked to interfacial protein-water relaxation, explain narrow lines of spectroscopic vibrational probes inside proteins.

As a medium for imbedded molecules and cofactors, proteins are characterized by highly dispersive dynamics with a nearly continuous distribution of relaxation times. A part of this phenomenology comes from confined and interfacial water, which demonstrates a nearly constant loss

(very slow power-law decay of the dielectric loss).[41] These conditions are responsible for glassy dynamics[42] when the time scale relevant for a specific process (observation time) falls into the spectrum of medium relaxation times thus making some of the relaxation modes dynamically frozen. As the observation time is altered by a protein-catalyzed reaction or instrumental resolution, the corresponding observables change nearly continuously because of the pseudocontinuous character of the relaxation spectrum.

This phenomenology is responsible for much studied dynamical transition in proteins[10,43] and for lowering barriers of electron-transfer reactions.[11] The same mechanism is also behind the recently discovered surprisingly high conductivity of proteins.[44] Likewise, slower dynamics of a confined protein lead to a stronger dynamical freezing and enhanced electrochemical response.[45] Overall, breaking the restrictions of the fluctuation-dissipation theorem by insufficient sampling might be a successful strategy, alternative to Pauling's stabilization of the activated state, for achieving the catalytic effect. In this view, not only the structure of the active site and the thermodynamic activation free energy, but also the relaxation time of the promoting mode determine function. Motions that matter for catalytic function must be faster than the reaction time. The free energy of activation loses its thermodynamic meaning and, instead, becomes a parameter affected by the placement of the reaction time within the relaxation spectrum of the medium. Specific details shaping this spectrum include the protein size, its confinement in the lipid membrane, and complex dynamics of electrostatic fluctuations of confined water and the protein-water interface. In the world of nonergodic sampling, dynamics become an additional parameter to tune catalytic function.[46]

This general perspective is applied here to formulate a phenomenological model of the vibrational line shape. We show that broadly observed[4] narrow vibrational lines in proteins can be attributed to slow dynamics of the electric field at the location of the probe. Most of the relaxation of the electric field occurs on the time scale far exceeding the lifetime of the excited vibrational state and is dynamically frozen. The corresponding inhomogeneous broadening is greatly reduced.

The vibrational line-width in a protein is often contrasted to that in water and the argument is put forward that the protein constrains fluctuations thus producing a medium with a low level of

electrostatic fluctuations (often connected to low polarity of proteins). In Figure 3, the line shape in the protein is contrasted with the line shape of the same vibrational probe in water (taken from ref 4) and to our calculation of the line shape in protein allowing full inhomogeneous broadening from electrostatic field fluctuations. It is clear that the protein is a medium with exceptionally strong electrostatic fluctuations. This observation connects the problem of line broadening with studies of charge transfer in proteins,[11] where similar claims of low polarity and small electrostatic noise at active sites were made. Similarly to our report here, fluctuations of electrostatic potential at active sites of enzymes are very large, leading to lowering of the activation barrier for charge transfer. Here, we likewise observe both very high average fields and strong fluctuations, which would make vibrational lines much broader if those fluctuations were allowed to contribute to inhomogeneous broadening. In water, fluctuations of similar magnitude are much faster and contribute to the line-width on the probe's lifetime. In short, both water and protein create strong electrostatic fluctuations, but proteins make a large fraction of them much slower.

Acknowledgement

This research was supported by the National Science Foundation (CHE-1800243). CPU time was provided by the National Science Foundation through XSEDE resources (TG-MCB080071).

Supporting Information Available

Description of the simulation protocol and of the analysis of electric field at protein carbonyls.

References

(1) Warshel, A.; Sharma, P. K.; Kato, M.; Xiang, Y.; Liu, H.; Olsson, M. H. M. Electrostatic basis for enzyme catalysis. *Chem. Rev.* **2006**, *106*, 3210–3235.

(2) Fried, S. D.; Bagchi, S.; Boxer, S. G. Extreme electric fields power catalysis in the active site of ketosteroid isomerase. *Science* **2014**, *346*, 1510–1514.

(3) Fried, S. D.; Boxer, S. G. Response to Comments on "Extreme electric fields power catalysis in the active site of ketosteroid isomerase". *Science* **2015**, *349*, 936–936.

(4) Fried, S. D.; Boxer, S. G. Electric fields and enzyme catalysis. *Annual review of biochemistry* **2017**, *86*, 387–415.

(5) Biava, H.; Schreiber, T.; Katz, S.; Völler, J.-S.; Stolarski, M.; Schulz, C.; Michael, N.; Budisa, N.; Kozuch, J.; Utesch, T. et al. Long-range modulations of electric fields in proteins. *J. Phys. Chem. B* **2018**, *122*, 8330–8342.

(6) Pauling, L. Molecular architecture and biological reactions. *Chem. Eng. News* **1946**, *24*, 1375–1377.

(7) Marcus, R. A.; Sutin, N. Electron transfer in chemistry and biology. *Biochim. Biophys. Acta* **1985**, *811*, 265–322.

(8) Kubo, R. The fluctuation-dissipation theorem. *Rep. Prog. Phys.* **1966**, *29*, 255–284.

(9) Henzler-Wildman, K. A.; Thai, V.; Lei, M.; Ott, M.; Wolf-Watz, M.; Fenn, T.; Pozharski, E.; Wilson, M. A.; Petsko, G. A.; Karplus, M. et al. Intrinsic motions along an enzymatic reaction trajectory. *Nature* **2007**, *450*, 838–844.

(10) Frauenfelder, H.; Chen, G.; Berendzen, J.; Fenimore, P. W.; Jansson, H.; McMahon, B. H.; Stroe, I. R.; Swenson, J.; Young, R. D. A unified model of protein dynamics. *Proc. Natl. Acad. Sci. USA* **2009**, *106*, 5129–5134.

(11) Matyushov, D. V. Protein electron transfer: is biology (thermo)dynamic? *J. Phys.: Condens. Matter* **2015**, *27*, 473001.

(12) Kubo, R. Note on the stochastic theory of resonance absorption. *J. Phys. Soc. Jpn.* **1954**, *9*, 935–944.

(13) Anderson, P. W. A Mathematical Model for the Narrowing of Spectral Lines by Exchange or Motion. *J. Phys. Soc. Jpn.* **1954**, *9*, 316–339.

(14) Fried, S. D.; Boxer, S. G. Measuring electric fields and noncovalent interactions using the vibrational Stark effect. *Acc. Chem. Res.* **2015**, *48*, 998–1006.

(15) Mukamel, S. *Principles of Nonlinear Optical Spectroscopy*; Oxford University Press: New York, 1995.

(16) Hamm, P.; Zanni, M. *Concepts and Methods of 2D Infrared Spectroscopy*; Cambridge University Press: Cambridge, UK, 2011.

(17) Oxtoby, D. Vibrational relaxation in liquids. *Ann. Rev. Phys. Chem.* **1981**, *32*, 77–101.

(18) Wang, M. C.; Uhlenbeck, G. E. On the theory of the Brownian motion II. *Rev. Mod. Phys.* **1945**, *17*, 323–342.

(19) Berne, B. J.; Pecora, R. *Dynamic Light Scattering*; Dover Publications, Inc.: Mineola, N.Y., 2000.

(20) la Cour Jansen, T.; Knoester, J. A transferable electrostatic map for solvation effects on amide I vibrations and its application to linear and two-dimensional spectroscopy. *J. Chem. Phys.* **2006**, *124*, 044502.

(21) Bakker, H. J.; Skinner, J. L. Vibrational Spectroscopy as a Probe of Structure and Dynamics in Liquid Water. *Chem. Rev.* **2009**, *110*, 1498–1517.

(22) Böttcher, C. J. F. *Theory of Electric Polarization, Vol. 1: Dielectrics in Static Fields*; Elsevier: Amsterdam, 1973.

(23) Seyedi, S. S.; Matyushov, D. V. Protein dielectrophoresis in solution. *J. Phys. Chem. B* **2018**, *122*, 9119–9127.

(24) Seyedi, S.; Matyushov, D. V. Dipolar susceptibility of protein hydration shells. *Chem. Phys. Lett.* **2018**, *713*, 210–214.

(25) Hansen, J.-P.; McDonald, I. R. *Theory of Simple Liquids*, 4th ed.; Academic Press: Amsterdam, 2013.

(26) Horch, M.; Schoknecht, J.; Wrathall, S. L. D.; Greetham, G. M.; Lenz, O.; Hunt, N. T. Understanding the structure and dynamics of hydrogenases by ultrafast and two-dimensional infrared spectroscopy. *Chem. Sci.* **2019**, *10*, 8981–8989.

(27) Bonner, G. M.; Ridley, A. R.; Ibrahim, S. K.; Pickett, C.; Hunt, N. Probing the effect of the solution environment on the vibrational dynamics of an enzyme model system with ultrafast 2D-IR spectroscopy. *Farad. Disc.* **2010**, *145*, 429–442.

(28) King, J. T.; Arthur, E. J.; Brooks III, C. L.; Kubarych, K. J. Site-specific hydration dynamics of globular proteins and the role of constrained water in solvent exchange with amphiphilic cosolvents. *J. Phys. Chem. B* **2012**, *116*, 5604–5611.

(29) Owrutsky, J. C.; Raftery, D.; Hochstrasser, R. M. Vibrational relaxation dynamics in solutions. *Ann. Rev. Phys. Chem.* **1994**, *45*, 519–555.

(30) Bagchi, B. *Molecular relaxation in liquids*; Oxford University Press: Oxford, 2012.

(31) Jimenez, R.; Fleming, G. R.; Kumar, P. V.; Maroncelli, M. Femtosecond solvation dynamics of water. *Nature* **1994**, *369*, 471.

(32) Cheng, Y.-K.; Rossky, P. J. Surface topography dependence of biomolecular hydrophobic hydration. *Nature* **1998**, *392*, 696–699.

(33) Laage, D.; Elsaesser, T.; Hynes, J. T. Water dynamics in the hydration shells of biomolecules. *Chem. Rev.* **2017**, *117*, 10694–10725.

(34) Qin, Y.; Zhang, L.; Wang, L.; Zhong, D. Observation of the Global Dynamic Collectivity of a Hydration Shell around Apomyoglobin. *J. Phys. Chem. Lett.* **2017**, *8*, 1124–1131.

(35) King, J. T.; Arthur, E. J.; Osborne, D. G.; Brooks III, C. L.; Kubarych, K. J. Biomolecular hydration dynamics probed with 2D-IR spectroscopy: From dilute solution to a macromolecular crowd. *Chinese Chemical Letters* **2015**, *26*, 435–438.

(36) Jordanides, X. J.; Lang, M. J.; Song, X.; Fleming, G. R. Solvation dynamics in protein environments studied by photon echo spectroscopy. *J. Phys. Chem. B* **1999**, *103*, 7995–8005.

(37) Bhattacharyya, K. Solvation dynamics and proton transfer in supramolecular assemblies. *Acc. Chem. Res.* **2003**, *36*, 95–101.

(38) Abbyad, P.; Shi, X.; Childs, W.; McAnaney, T. B.; Cohen, B. E.; Boxer, S. G. Measurement of solvation responses at multiple sites in a globular protein. *J. Phys. Chem. B* **2007**, *111*, 8269–8276.

(39) Seyedi, S.; Waskasi, M. M.; Matyushov, D. V. Theory and electrochemistry of cytochrome *c*. *J. Phys. Chem. B* **2017**, *121*, 4958–4967.

(40) Martin, D. R.; Matyushov, D. V. Dipolar nanodomains in protein hydration shells. *J. Phys. Chem. Lett.* **2015**, *6*, 407–412.

(41) Ngai, K. L.; Capaccioli, S.; Ancherbak, S.; Shinyashiki, N. Resolving the ambiguity of the dynamics of water and clarifying its role in hydrated proteins. *Phil. Mag.* **2011**, *91*, 1809–1835.

(42) Stillinger, F. H.; Debenedetti, P. G. Glass transition thermodynamics and kinetics. *Annu. Rev. Condens. Matter Phys,* **2013**, *4*, 263–285.

(43) Seyedi, S.; Matyushov, D. V. Ergodicity breaking of iron displacement in heme proteins. *Soft Matter* **2017**, *13*, 8188–8201.

(44) Zhang, B.; Song, W.; Brown, J.; Nemanich, R.; Lindsay, S. Electronic conductance resonance in non-redox-active proteins. *J. Am. Chem. Soc.* **2020**, *142*, 6432–6438.

(45) Samajdar, R. N.; Asampille, G.; Atreya, H. S.; Bhattacharyya, A. J. Hemoglobin dynamics in solution vis – à – vis under confinement – An electrochemical perspective. *J. Phys. Chem. B* **2020**, ASAP acs.jpcb.0c02372.

(46) Matyushov, D. V. Fluctuation relations, effective temperature, and ageing of enzymes: The case of protein electron transfer. *J. Molec. Liq.* **2018**, *266*, 361–372.